A Cell-Based Traffic Control Formulation: Strategies and Benefits of Dynamic Timing Plans

Hong K. Lo
Department of Civil Engineering, Hong Kong University of Science and Technology, Clear Water Bay, Hong Kong, People's Republic of China

This study developed a dynamic traffic-control formulation that considers the entire Fundamental Diagram. This incorporation of the Fundamental Diagram is especially important for modeling oversaturated traffic. For this purpose, traffic is modeled after the cell-transmission model (CTM), which is a convergent numerical approximation to the hydrodynamic model. We transformed CTM to a set of mixed-integer constraints and subsequently cast the dynamic signal-control problem to a mixed-integer linear program. As a dynamic platform, the formulation is flexible in dealing with dynamic timing plans and traffic patterns. It can derive dynamic as well as fixed timing plans and address preexisting traffic conditions and time-dependent demand patterns. This study produced results to show the benefit of dynamic timing plans and demonstrated that some of the existing practice on signal coordination could be further improved.

1. Introduction

It is well accepted that vehicular traffic follows a concave flow-density relationship as shown in Figure 1. In this relationship, often referred to as the Fundamental Diagram, the left-hand side between $k = 0$ to $k = k_o$ represents the regime of normal or stable flow (Khisty and Lall 1998, McShane et al. 1998). Primarily, the demand determines the flow—the higher the demand, the higher the flow. When the demand exceeds the capacity, Qmax, traffic is represented by the right side between $k = k_o$ to k_{jam}, sometimes called the regime of forced flow (Khisty and Lall 1998, McShane et al. 1998). The system operates at a high density but low flow, which is an inefficient mode of operation. In the extreme case of $k = k_{jam}$, a gridlock is formed in which the flow becomes essentially zero and the roadway acts like a filled parking lot. Due to its concave shape, each flow has two possible densities: one in the normal flow regime, the other in the forced flow regime. Therefore, to fully specify a particular traffic condition, both its flow and density must be stated.

This fundamental relationship of traffic flow provides vital information to determine optimal signal-control plans, especially for traffic that is in the forced flow or oversaturated regime. To illustrate the point, let's consider that a heavy demand creates the initial traffic state "$(f, k2)$" in Figure 1, where the flow is low and the density is high. It should be clear from Figure 1 that the most efficient way to clear the heavy demand is to operate the system at $k = k_o$, sometimes called the optimum density, which has the highest flow rate. Thus, the optimal strategy to clear the oversaturated traffic is to modify the traffic density through coordinated metering, from k2 to k0. Though simple, this concept is rarely applied in existing signal-control models. An example is found in Papageorgiou et al. (1990), although that study focused on freeway ramp metering. Indeed, unless traffic is modeled through the Fundamental Diagram, it would be difficult for a signal-control model to

Transportation Science © 2001 INFORMS
Vol. 35, No. 2, May 2001 pp. 148–164
0041-1655/01/3502/0148$05.00
1526-5447 electronic ISSN

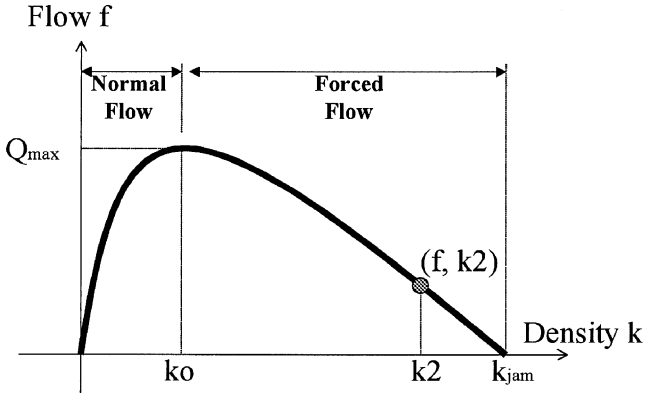

Figure 1 The Fundamental Flow-Density Relationship

modify the traffic density so as to arrive at that maximum flow.

Moreover, without the Fundamental Diagram, it would be difficult to obtain accurate queue length estimations for oversaturated traffic (Stephanopoulos et al. 1979). They argued that frequent stop-and-go movements generate complicated traffic dynamics in the form of shockwaves. Density along the queue length is constantly in a state of transition, which renders the assumption of compact queue and constant average density questionable. Therefore, the customary approach of estimating the queue length (in meters) from the queue size (in number of queued vehicles), and the average distance occupied by a vehicle, is inadequate. In short, without the Fundamental Diagram, a model could not provide a good description of queue dynamics in heavy congestion.

Information on queue dynamics is vital in determining timing plans for oversaturated traffic. Ideally, the plans should be timed such that every green second should be serving traffic at its maximum flow rate. It is suboptimal to have a green signal serving an empty link or to generate the situation that the waiting traffic is stopped by a downstream blockage during a green signal, in a phenomenon called de facto red. Due to the dynamic nature of queuing in oversaturated traffic, the lengths of the green times must be able to adjust dynamically with the queues. Thus, one must determine dynamic, as opposed to fixed, timing plans to handle oversaturated traffic. In fact, part of the numerical study reported herein is to demonstrate such needs by comparing their performance under various loading situations.

Therefore, these two ingredients are important for controlling oversaturated traffic or the regime of forced flow, namely the Fundamental Diagram and dynamic timing plans. When traffic is in the normal flow regime, however, the benefit of including the Fundamental Diagram is not as apparent even though it is still applicable. Firstly, there is no need to modify the density or flow rate, as they are predominantly determined by the demand, not the capacity. Secondly, most of the traffic can be cleared within one cycle. Queue spillback across multiple links and/or cycles is not a problem. To simplify the analysis, one may assume that traffic repeats itself in a cyclic manner; hence, optimizing a set of fixed timing plans is sufficient. One may also use the results of classical queuing theory (which does not consider traffic density and speed variations) to represent the effect of a signal-timing plan. The fundamental principles and possible extensions of this approach can be found in Newell (1989).

A comprehensive review of most of the commonly used traffic control systems is provided in Wood (1993). As contended earlier, for traffic in the regime of normal flow, these models perform well and have been used extensively in practice. To cite some examples, TRANSYT-7F Version 7 (Courage and Wallace 1991) remains a popular software to determine fixed timing plans. It uses an empirically based platoon dispersion model to produce cyclic flow profiles (CFP) for each link. For simplicity, the vehicles are treated as moving freely to the stopline and joining a vertical queue there. For congested situations, this assumption might produce results such that the queue length is longer than the length of the link. The most recent version, TRANSYT-7F Release 8 (Wallace et al. 1998), added abilities to overcome this shortcoming and to consider oversaturated traffic. Several refinements were introduced: (i) more accurate calculation of the back of queues; (ii) placing arrivals at the back of the queue rather than at the stopline; (iii) permitting different cycle lengths for uncoordinated intersections; and (iv) extending the simulation from "single-cycle" to "multi-cycle." Its fundamental approach—using the platoon dispersion model to produce CFP and

determining fixed time plans—remains unchanged, however. Moreover, since traffic density is not an input, it would be difficult for TRANSYT-7F to work with initial traffic states in the forced-flow regime, say (f, $k2$) in Figure 1. Also aimed at determining fixed time plans are MAXBAND (Little et al. 1981) and PASSER (TTI 1991). These programs calculate plans to produce good progression along main arterials by optimizing the green bandwidth. Gartner et al. (1991) extended this concept to a multiband approach by determining the individual bandwidths for each directional link. Indeed, the level of sophistication of these models has been greatly refined over the years. Nevertheless, to our knowledge, none of the existing traffic signal models incorporates the Fundamental Diagram in their traffic models.

There are also signal-control models developed specifically for oversaturated traffic. Gazis (1964) was the first study that formulated the problem of signal control for oversaturated traffic, which was subsequently extended by D'Ans and Gazis (1976) to propose a "store-and-forward" approach. Michalopoulos and Stephanopoulos (1977) further extended Gazis' model by introducing the queue length constraints. Recently, a number of other formulations were proposed, such as Eddelbuttel and Cremer (1994), Abu-Lebdeh and Benekohal (1997), and Wey and Jayakrishnan (1997). They all modeled traffic as a queuing network. Some added explicit constraints to avoid de facto red. These models provide timing plans for queue management by containing the queue spillback and avoiding blockage. Nevertheless, the notion of modifying traffic density to the optimum level is not included, nor is the Fundamental Diagram considered.

In this paper, we develop a dynamic traffic-signal-control formulation that includes the entire Fundamental Diagram as its traffic model. Both the regimes of normal flow and forced flow are included in this consideration. Theoretically, it is able to work with the whole range of traffic conditions covered by the Fundamental Diagram. Several approaches are available to incorporate the Fundamental Diagram in a traffic flow model. The first is a microscopic approach that uses car-following conditions to simulate vehicle movements, such as the GM models (May 1990). Solution speed of this approach could be a concern when applied to signal-control problems. However, recent advances, such as cellular automata (CA) (Nagel and Schreckenberg 1992), seem to have improved the computational efficiency of this approach substantially. The second approach is macroscopic in nature. Lighthill and Whitham (1955) and Richards (1956) (the LWR model) provided a good foundation. Until recently, solution difficulty has prevented the use of the LWR model for signal control. A breakthrough came when Daganzo (1994, 1995) developed a finite difference solution scheme for the LWR model by adopting a simplified Fundamental Diagram, which he called the cell-transmission model (CTM). Such a model is a possible candidate.

Recently, there has been a resurgence of interest in the Fundamental Diagram and the associated dynamic traffic flow models (for example, see Lebacque and Lesort (1999) for a brief summary). The issues on the order of the models, the effect of acceleration and dispersion, and the extensions to multi-user classes are just some examples of the topics being considered and reexamined. Many of these questions are still unsettled and remain research challenges. For our purpose here, we merely emphasize the importance of the Fundamental Diagram for traffic-signal control and provide an approach to demonstrate the benefit of doing so. We leave the effects of different Fundamental-Diagram-based traffic flow models on the control scheme to a future study. At this moment, we do not anticipate substantial changes to the general results of the control strategies demonstrated in the numerical study of this paper. However, second-order details may be different. Nonetheless, it is hoped that the technique developed herein would also be useful for incorporating other dynamic traffic flow models.

For simplicity, this study chooses CTM as the underlying dynamic traffic flow model. The LWR model, and hence CTM, are referred to as the first-order models. Despite their simplicity (when compared with the higher-order models), field data suggested that they fit measurements well. See for example, Lin and Ahanotu (1995) and Smilowitz and Daganzo (1999). These two studies validated CTM

for freeway and arterial traffic. In Chang (1998), we collected extensive delay data on signalized urban streets, and validated that CTM's delay estimates matched reasonably with the actual field measurements under a variety of traffic conditions. This result established CTM as a plausible model for signalized urban streets.

In this paper, we develop an approach to transform CTM to a set of mixed-integer linear constraints in a mathematical program (MP). The significance of this is that the transformed CTM (and hence, the underlying LWR model) can now be used for a general optimization context, such as the dynamic signal control developed herein, dynamic traffic assignment (Lo 1999a), or other optimization problems that include a traffic model. This transformation of CTM, however, is not straightforward. CTM, intended for simulation-based operations, includes operators that could not be directly incorporated as constraints. This study develops a technique to convert CTM to a set of mixed-integer constraints. This transformation, however, increases the complexity of the formulation. In particular, solving this mixed-integer program is computationally intensive. For demonstration purposes, this study uses a small network to illustrate the solution quality. We recognize that applying this formulation to real-sized networks would require the development of heuristics for solutions. An example of its application to a real network based on the heuristic of genetic algorithms can be found in Lo et al. (2001).

The outline of this paper is the following. Section 2 depicts a brief summary of CTM together with the mixed-integer programming formulation. Section 3 presents the numerical study and results. We construct several scenarios ranging from light to gridlock traffic to show the capability of this formulation. As a dynamic formulation, it can handle both fixed as well as dynamic timing plans. We will show the benefit of dynamic timing plans. The results show that some of the existing practices on signal coordination can be further improved. Finally, §4 provides some concluding remarks.

2. Formulation

2.1. The Cell-Transmission Model

The Lighthill and Whitham (1955) and Richards (l956) (LWR) model can be stated by the following two conditions:

$$\frac{\partial f}{\partial x}+\frac{\partial k}{\partial t}=0 \quad \text{and} \quad f=F(k,x,t) \tag{1}$$

where f is the traffic flow; k is the density; x and t, respectively, are the space and time variables; and F is a function relating f and k. The first partial differential equation states the traffic flow conservation condition. The relation F between flow f and density k defines the Fundamental Diagram. Given a set of well-posed initial conditions, one can determine f and k at any (x,t) by solving (1). This model is sometimes referred to as the hydrodynamic or kinematic wave model of traffic flow. Lighthill and Whitham (1955) and Newell (1991) developed two different solution approaches to this model. Daganzo (1994, 1995) simplified the solution scheme by adopting the following relationship between traffic flow, f, and density, k:

$$f=\min\{Vk, Q, W(k_{\text{jam}}-k)\} \tag{2}$$

where k_{jam}, Q, V, W denote, respectively, jam density, inflow capacity (or maximum allowable inflow), free-flow speed, and the speed of the backward shock wave (or the backward propagation speed of disturbances in congested traffic); then the LWR equations for a single highway link are approximated by a set of difference equations. Essentially, (2) approximates the Fundamental Diagram by a piecewise linear model, as shown in Figure 2.

By discretizing the road into homogeneous sections (or cells) and time into intervals such that the cell

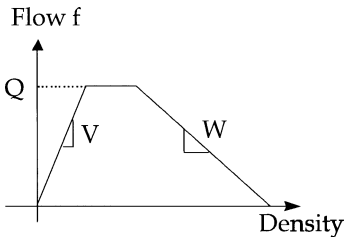

Figure 2 The Flow-Density Relationship Used in CTM

length is equal to the distance traveled by free-flowing traffic in one time interval, then the LWR results are approximated by this set of recursive equations (Daganzo 1994, 1995):

$$n_j(t+1) = n_j(t) + f_j(t) - f_{j+1}(t) \quad (3)$$

$$f_j(t) = \min\{n_{j-1}(t), Q_j(t), \quad (W/V)[N_j(t) - n_j(t)]\} \quad (4)$$

where the subscript j refers to cell j, and $(j+1)$, $(j-1)$ represents the cell downstream (upstream) of j. The variables $n_j(t)$, $f_j(t)$, $N_j(t)$ denote the number of vehicles, the actual inflow, and the maximum number of vehicles (or holding capacity) that can be present in cell j at time t, respectively. The variables $Q_j(t)$, V, W follow the earlier definitions. It is important to differentiate between $Q_j(t)$ and $f_j(t)$: The former is the inflow capacity while the latter is the actual inflow. Because (3)–(4) provide a numerical approximation to the LWR equations, all the traffic phenomena demonstrated in the LWR model, such as kinematic waves, are replicated in CTM.

As a first-order model, CTM does not consider traffic dispersion in free-flow traffic. Light traffic is modeled to move forward in a platoon as determined by the inflow demand. In the absence of a signal or downstream congestion, this platoon will maintain the same density without dispersion. Under these circumstances, the effect of the green time in clearing traffic might be overestimated. In congested traffic or short urban streets typically found in city centers, the opportunities and extent of free-flow dispersion would be smaller; movements are predominantly restricted by the downstream traffic or signal. CTM does model the speed at which space is opening up from the downstream for the upcoming traffic, via the ratio of the shock wave to free-flow speeds or the third term on the right-hand side in (4). In this sense, traffic dispersion in the form of density variation is considered at the merge of two traffic streams. This simplification in ignoring free-flow dispersion is a potential limitation that deserves further analysis. As far as estimating delay is concerned, Chang (1998) validated that CTM's delay estimates on signalized urban streets matched well with the actual measurements in both light and congested traffic.

2.2. The Cell-Based Traffic Dynamics Representation

We consider a network consisting of a main corridor intersecting with a number of cross streets. To simplify the exposition, turning movements are prohibited in this network. Relaxing this limitation is possible, as demonstrated in Lo et al. (2001). We classify links into three types:

- source link, denoted by set Ω—where traffic enters the network
- exit link, denoted by set E—where traffic exits the network,
- intermediate link, denoted by link set Ψ—which is neither a source nor exit link.

Each link is subdivided into cells. The cells in each link are numbered consecutively from the upstream direction and follow this nomenclature: cell(i, j) represents the jth cell in link i. Except the cells with special characteristics as discussed below, all the cells are assigned a set of identical characteristics, including: $N_{ij}(t)$—holding capacity (assumed to be time-invariant in this study, so the time dimension can be dropped); $Q_{ij}(t)$—inflow capacity; V—free-flow speed; and W—backward shock wave speed.

The first cell of a source link acts like a big parking lot; it stores the total demand that is scheduled to enter the network. The rate at which dynamic demand enters the source link is set by the inflow capacity of the second cell. Vehicles will enter the network according to the demand if space is available in the second cell. Otherwise, vehicles will wait in the big parking lot. Mathematically,

$$n_{i1}(1) = \sum_t D_i(t), \quad i \in \Omega \quad (5)$$

$$Q_{i2}(t) = D_i(t), \quad i \in \Omega \quad (6)$$

where $n_{i1}(1)$ denotes the number of vehicles in cell$(i, 1)$ at time $t = 1$; $D_t(t)$ the exogenous dynamic demand to source link i at time t; and $Q_{i2}(t)$ the inflow capacity of cell $(i, 2)$ at time t.

For the intermediate links, the first cell is modeled to function like a traffic signal. That is,

$$Q_{i1}(t) = \begin{cases} s & \text{if } t \in \text{green phase} \\ 0 & \text{if } t \in \text{red phase} \end{cases}, i \in \Psi \quad (7)$$

where s is the saturation flow and $Q_{i1}(t)$ is the inflow capacity of link i.

The exit links are modeled to have only one cell. This cell serves two purposes. Firstly, it simulates the action of a signal, as in (7). Secondly, it serves as a reservoir to store all the vehicles that exit from the network, and is used to show the arrival flows. Its holding capacity is set to infinity in order not to restrict vehicle arrival. (The effect of limited space at the exit of a network can be introduced by assigning a finite capacity.) That is,

$$N_{i1}(t) = \infty, \quad i \in \mathrm{E} \tag{8}$$

2.3. Delay Estimation

This cell-based approach provides a convenient way to determine delay. Delay here is defined as the additional time beyond the nominal or free-flow travel time a vehicle stays in a cell. At the cell level, the delay is determined as:

$$d_{ij}(t) = n_{ij}(t) - f_{i,\,j+1}(t) \tag{9}$$

Basically, if the exit flow from cell (i, j) at time t is less than its current occupancy due to congestion, those who cannot leave the cell will incur a delay of one time step. Once the delay has been determined at the cell level, it can be easily aggregated at the link or network level.

2.4. Mixed-Integer Signal-Control Program

Traffic-signal control serves many purposes, and therefore many objective functions are possible. One may choose to minimize delay, the total number of slowed-down vehicles, or a combination of these, or to maximize the total outflow from the network. All of these are possible with this formulation. For simplicity and illustration purposes, this study chooses to minimize the common measure of total network delay:

$$J = \min \sum_t \sum_i \sum_j d_{ij}(t), \tag{10}$$

where $d_{ij}(t)$ is defined in (9). The objective is to select the duration of the signal phases such that J is minimized. This minimization is subject to the constraints of exogenous dynamic demand, traffic dynamics according to CTM, and the minimum and maximum durations of red and green times commonly adopted in practice.

(A) *Exogenous Demand.*

$$Q_{i2}(t) = D_i(t) \quad i \in \Omega \tag{11}$$

where $D_i(t)$ is the exogenous dynamic demand to source link i.

(B) *Traffic Dynamics According to CTM.* In networks without turning movements, CTM uses two equations (3)–(4) to describe traffic flow. Constraint (3) can be part of the constraint set directly. However, (4) is nonlinear due to the embedded minimization. Its direct inclusion as constraints would make the program difficult to solve. A simple way to avoid this nonlinear constraint is to replace it with three less-than constraints (Lo 1999b):

$$f_{ij}(t) \le n_{i,\,j-1}(t) \tag{12}$$

$$f_{ij}(t) \le Q_{ij}(t) \tag{13}$$

$$f_{ij}(t) \le \left(\frac{W}{V}\right)[N_{ij}(t) - n_{ij}(t)] \tag{14}$$

This simplification removes the nonlinearity of (4). However, the constraints (12)–(14) cannot guarantee that $f_{ij}(t)$ assumes the same minimum as (4). For example, $f_{ij}(t) = 0$ remains a feasible solution to (12)–(14), even though the right-hand sides of (12)–(14) are all greater than zero. This phenomenon can be described as the "vehicle-holding" problem, which should not occur in reality. In this study, we overcome this problem by introducing a more complex formulation to linearize (4). Each instance of (4) requires six constraints and two binary variables for its full representation. To simplify notations, let:

$$f(\cdot) = f_{ij}(t);\ \ n(\cdot) = n_{i,\,j-1}(t);$$

$$Q(\cdot) = Q_{ij}(t);\ \ h(\cdot) = \frac{W}{V}[N_{ij}(t) - n_{ij}(t)],$$

and let y_i, $i = 1, 2$ be two binary variables. The minimization (4) can be divided into two steps:

$$f(\cdot) = \min\{\phi(\cdot), h(\cdot)\} \tag{15}$$

$$\text{and } \phi(\cdot) = \min\{n(\cdot), Q(\cdot)\} \tag{16}$$

Condition (16) can be equivalently stated as this set of linear constraints:

$$L(1-y_1) \le n(\cdot) - Q(\cdot) \le U \cdot y_1 \tag{17}$$

$$0 \le n(\cdot) - \phi(\cdot) \le U \cdot y_1 \tag{18}$$

$$0 \le Q(\cdot) - \phi(\cdot) \le U(1-y_1) \tag{19}$$

where L is a very large negative constant, and U a very large positive constant. To illustrate the effect of these constraints, we substitute the only two possible values of y_1 into (17)–(19) to obtain:

$$y_1 = 1 \iff \left\{ \begin{array}{l} 0 \le n(\cdot) - Q(\cdot) \le U \iff Q(\cdot) \le n(\cdot) \\ 0 \le n(\cdot) - \phi(\cdot) \le U \iff \phi(\cdot) \le n(\cdot) \\ 0 \le Q(\cdot) - \phi(\cdot) \le 0 \iff \phi(\cdot) = Q(\cdot) \end{array} \right\}$$

$$\iff \text{set } \phi(\cdot) = Q(\cdot) \text{ for } Q(\cdot) \le n(\cdot)$$

$$y_1 = 0 \iff \left\{ \begin{array}{l} L \le n(\cdot) - Q(\cdot) \le 0 \iff n(\cdot) \le Q(\cdot) \\ 0 \le n(\cdot) - \phi(\cdot) \le 0 \iff \phi(\cdot) = n(\cdot) \\ 0 \le Q(\cdot) - \phi(\cdot) \le U \iff \phi(\cdot) \le Q(\cdot) \end{array} \right\}$$

$$\iff \text{set } \phi(\cdot) = n(\cdot) \text{ for } n(\cdot) \le Q(\cdot)$$

In essence, the binary variable y_1 captures the only two possibilities: Namely, set the minimum $\phi(\cdot)$ to $Q(\cdot)$ if $Q(\cdot)$ is smaller, otherwise, set $\phi(\cdot)$ to $n(\cdot)$. Thus, the minimization (16) can be replaced by the linear constraints (17)–(19). Repeating the same logic, (15) can be stated equivalently by:

$$L(1-y_2) \le \phi(\cdot) - h(\cdot) \le U \cdot y_2 \tag{20}$$

$$0 \le \phi(\cdot) - f(\cdot) \le U \cdot y_2 \tag{21}$$

$$0 \le h(\cdot) - f(\cdot) \le U(1-y_2) \tag{22}$$

Likewise, one can verify that $f(\cdot) = h(\cdot)$ if and only if $y_2 = 1$, and $f(\cdot) = \phi(\cdot)$ if and only if $y_2 = 0$. In summary, traffic flow according to CTM is represented by the linear constraints (3) and (17)–(22).

(C) *Control Decisions.* In networks without turning, there are only two phases at each junction, either green (red) for the main corridor (cross-street) traffic, or vice versa. This study further assumes that cycle time is fixed. This assumption is merely to reduce the solution time. As a dynamic platform, one can easily choose to relax this assumption by making the cycle time another decision variable in addition to the green time in each phase, or one can go further by choosing both the red and green phases as decision variables. In this last scenario, one basically removes the concept of a "cycle," and the formulation will be truly flexible in determining the length of each phase. The consideration here is the trade-off between solution flexibility/quality and solution time. In fact, the numerical study of this paper is partly to illustrate the benefit of relaxing some of these constraints on the decision variables.

So, with the assumption of fixed cycle time, the two types of decision variables are the offset and length of green time in each cycle. Offset is defined to be the time from the start of the modeling horizon ($t = 1$) to the start of the first green and is set to red (green) for the main corridor (cross-street) traffic. With fixed cycle time, the red time can be determined given the green time in the same cycle. Following the common practice, both green and red times are restricted by upper and lower bounds. That is,

$$R_{\min} \le \theta_a \le R_{\max} \tag{23}$$

$$G_{\min} \le g_a(l) \le G_{\max} \tag{24}$$

where θ_a is the initial offset for the main corridor at intersection a. The variables $R_{\max}$ and $R_{\min}$ denote the maximum and minimum red time, and $G_{\max}$, $G_{\min}$, $g_a(l)$ denote, respectively, the maximum and minimum green time, and the green time for the main corridor at intersection a in cycle l. This formulation includes the fixed timing plans as a special case by setting $g_a(l)$ to be the same decision variable for all cycles.

Choosing θ_a, $g_a(l)$ as the decision variables, it is necessary to relate them to the inflow capacity, $Q_{i1}(t)$, of the first cell of each signalized link. Basically, when the signal for an approach is green (red), its inflow capacity is equal to the saturation flow (zero). To this end, the phases are numbered at each intersection consecutively (Figure 3).

To illustrate how a signal phase is related to inflow capacities, we consider the case of phase p in cycle l at intersection a. Let's assume that p is an even number and, hence, a green phase for the major approach. Other phases and intersections can be constructed

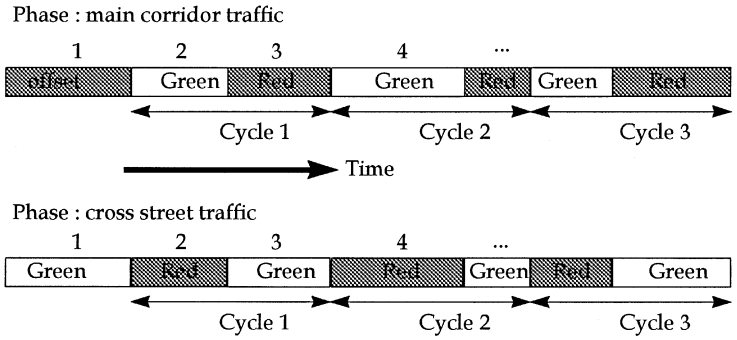

Figure 3 The Phase Numbers

in a similar way. At intersection a, let m, n be the signalized links on the main corridor and the cross street, respectively. Thus, the signalized cell on the main corridor is cell$(m, 1)$, while the signalized cell on the cross street is cell$(n, 1)$. For ease of exposition, we drop subscript "a" from the variable notations. Choosing the lengths of the first offset θ and the green phase $g(l)$ as the decision variables, the start and end times of that phase, $S(p)$, $E(p)$, are, respectively:

$$S(p) = \theta + (l-1)C \tag{25}$$

$$E(p) = S(p) + g(l) \tag{26}$$

where l defines the cycle that contains p. The inflow capacities for this phase are:

$$\text{if } S(p) < t \le E(p), \text{ then } \begin{cases} Q_{m1}(t) = s \\ Q_{n1}(t) = 0 \end{cases} \tag{27}$$

As an "if-then" condition, (27) cannot directly be part of the constraint set. All the constraints of a mathematical program must hold *simultaneously*, not conditionally. To capture the effect of (27), we develop the following mixed-integer technique. Firstly, we identify for each time t whether it falls in this phase or not. Then, according to this result, we set the inflow capacity of the signalized cell at time t to either the saturation flow or zero. This procedure is accomplished with three binary variables: $y_1(p, t), y_2(p, t), z(t)$. The variable $y_1(p, t)$ checks whether the condition $t \le E(p)$ is satisfied. If so, set $y_1(p, t) = 1$; otherwise, set $y_1(p, t) = 0$. Similarly, the second binary variable checks the condition $t > S(p)$. Set $y_2(p, t) = 1$ if so; set $y_2(p, t) = 0$ otherwise. The third binary variable $z(t)$ allocates the appropriate inflow capacities to the signalized cells according to the values of $y_1(p, t), y_2(p, t)$. The corresponding set of linear constraints can be stated as:

$$-U \cdot y_1(p, t) + \varepsilon \le t - E(p) \le U \cdot [1 - y_1(p, t)] \tag{28}$$

$$-U \cdot y_2(p, t) \le S(p) - t \le U \cdot [1 - y_2(p, t)] - \varepsilon \tag{29}$$

$$y_1(p, t) + y_2(p, t) - z(t) \le 1 \tag{30}$$

$$Q_{m1}(t) = z(t) \cdot s \tag{31}$$

$$Q_{n1}(t) = [1 - z(t)] \cdot s \tag{32}$$

where U is a very large constant and ε is a very small constant. If one substitutes the two possible values of $y_1(p, t)$ into (28), one would find the following result:

$$y_1(p, t) = 1 \Longleftrightarrow -U + \varepsilon \le t - E(p) \le 0 \Longleftrightarrow t \le E(p)$$

$$y_1(p, t) = 0 \Longleftrightarrow \varepsilon \le t - E(p) \le U \Longleftrightarrow t > E(p)$$

Thus, constraint (28) correctly captures the relationship between $y_1(p, t)$ and the condition $t \le E(p)$. In a very similar way, one can verify that constraint (29) correctly captures the condition $t > S(p)$. That is,

$$y_2(p, t) = 1 \Longleftrightarrow -U \le S(p) - t \le -\varepsilon \Longleftrightarrow t > S(p)$$

$$y_2(p, t) = 0 \Longleftrightarrow 0 \le S(p) - t \le U - \varepsilon \Longleftrightarrow t \le S(p)$$

If both $y_1(p, t)$ and $y_2(p, t)$ equal 1, then $S(p) < t \le E(p)$ or time t lies within phase p. Otherwise, t is in some other phase. Substituting this result into (30)–(32), one has:

$$\begin{cases} y_1(p, t) = 1 \\ y_2(p, t) = 1 \end{cases} \Longleftrightarrow z(t) \ge 1 \Longleftrightarrow z(t) = 1 \Longleftrightarrow \begin{cases} Q_{21}(t) = s \\ Q_{51}(t) = 0 \end{cases}$$

This produces the required result. For each of the phases in the modeling horizon, we repeat this procedure and construct a set of similar mixed-integer linear constraints. Each set of constraints transforms the signal states to the inflow capacities for t's that lie in that phase. Moreover, by constructing the sets of constraints such that each t lies in exactly one phase, there will be no conflict in assigning the value of $z(t)$.

The size of this mixed-integer linear program grows linearly with the network size and the modeling horizon. Let T be the number of time steps in the modeling horizon. Each cell requires $2T$ binary variables and $7T$ constraints [(3), (17)–(22)]. Each signal phase requires $3T$ binary variables and $7T$ constraints [(25)–(26), (28)–(32)]. With fine time steps and a long modeling horizon, this mixed-integer problem can be tedious to solve.

3. Numerical Study of Performance

3.1. Study Design

The objective of this numerical study is to demonstrate the applicability of this formulation for different traffic conditions. Since this dynamic formulation can derive both fixed and dynamic timing plans, the second objective is to investigate the benefits of adopting a dynamic as compared to a static approach. It is hoped that some of the strategies generated by this dynamic approach would shed light on improving some of the practices. To this end, small tractable examples are preferable. Thus, we use the network shown in Figure 4 for this study.

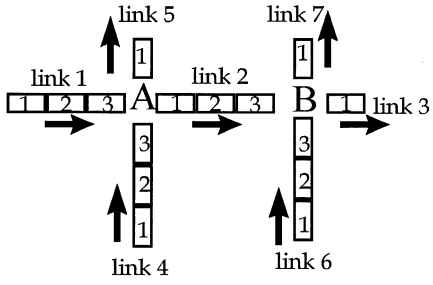

Figure 4 The Network for the Numerical Study

The input parameters include:

- All links have 1 lane;
- Free-flow speed: 50 km/h;
- Backward shock wave speed: 50 km/h;
- Jam density: 120 vehicles/km (equivalent to 16.67 vehicles/cell);
- Optimum density: 36 vehicles/km (equivalent to 5 vehicles/cell);
- Saturation flow: 1800 vehicles/hour (equivalent to 5 vehicles/time step);
- Time step: 10 seconds;
- Cycle time: 40 seconds;
- Minimum green and red time: 10 seconds;
- Maximum green and red time: 30 seconds;
- Modeling horizon: 6 cycles (equivalent to 4 minutes or 24 time intervals).

This formulation works for the full range of traffic conditions. Thus, we set up four demand scenarios to test its performance:

- Scenario 1 has a heavy demand of 1800 vph on the main corridor and light demands of 360 vph on the cross streets. The network is empty initially.
- Scenario 2 has a heavy demand of 1800 vph on the main corridor. The demands on the cross streets are uneven: 180 vph on Link 4, 1800 vph on Link 6. The network is initially empty.
- Scenario 3 has a heavy demand of 1800 vph on the main corridor and lighter demands of 360 vph on the cross streets. The entire network is preloaded at the jam density initially.
- Scenario 4 has a heavy demand of 1800 vph on the main corridor and heavy demands of 900 vph on the cross streets. The entire network is preloaded at half the jam density initially.

Table 1 summarizes these demand scenarios.

3.2. Results

By definition, the timing plans generated by this formulation minimize the system delay for the given demand and initial loading conditions. To understand the strategies of these plans, we prepare Tables 2–5. In each table, the first column indicates the time steps. Columns 5 and 9 show the signal states at intersections A and B, respectively. "XX" indicates red; "—" indicates green. Column 2 shows the total demand

Table 1 Dynamic Demands of the Four Scenarios

Scenario	Initial Condition	Loading Duration (Time Steps)	Demand/Time Interval (Vehicles/Time Step)		
			Link 1	Link 4	Link 6
1	Empty network	$1 \le t \le 24$	5.0	1.0	1.0
2	Empty network	$1 \le t \le 24$	5.0	0.5	5.0
3	All links at jam density	$1 \le t \le 5$	5.0	1.0	1.0
		$6 \le t \le 24$	0.0	0.0	0.0
4	All links at half the jam density	$1 \le t \le 5$	5.0	2.5	2.5
		$6 \le t \le 24$	0.0	0.0	0.0

Note. 1 veh/time step is equivalent to 360 veh/hr. Hence, 5 veh/time step (or 1800 veh/hr) is the capacity of the roadway.

intended to enter the network. The last column indicates vehicles that left the network. Other entries in these tables depict the number of vehicles (rounded to integer) in each cell in each time step. Blank cells indicate empty cells. Because of space limitations, we present results only for the major arterial, along Links 1, 2, and 3. The average delays per exit vehicles for the different scenarios are provided in Table 6.

Tables 2–5 show that green progression is the best strategy under a variety of demand conditions. This strategy works for the lighter-demand scenarios 1 and 2 as well as for the heavy-demand scenarios 3 and 4. While it is relatively simple to create green progressions for the lighter-demand scenarios, doing so for the heavy-demand scenarios with preexisting traffic is not straightforward. An examination of the dynamic plans of scenarios 3 and 4 (Tables 4 and 5) show that during the early time steps, the downstream junction released traffic at the maximum rate and the upstream junction metered traffic at the minimum rate. Eventually, when the traffic density in cells of Link 2 was lowered to the optimum density (five per cell), the plan switched to forward progression. Green progression is the best strategy because it "delivers" vehicles to the downstream junction just on time for the green signal. For the main corridor, one second of delay on Link 1 is the same as one second of delay on Link 2. Therefore, a timing plan that allows an accumulation of vehicles on Link 2 would not benefit the main corridor. Doing so, however, would hurt the cross street on the first junction. Instead, the cross street at the first junction can use more green time to clear traffic.

Table 3 shows the results for Scenario 2. Despite the fact that the demands on the cross streets are very different (a factor of 10, 180 vph versus 1800 vph), the fixed timing plan allocated the same green time (actually the maximum green) to the main corridor at both junctions. Had the green times been determined at the junction level in an isolated manner, one would not obtain this optimal fixed plan. This shows that cross-street demands of neighboring junctions would have an influence in green time allocation. The reasoning behind this is that a corridor's throughput is restricted by its bottleneck. To a certain extent, the green allocation at the bottleneck dictates the green allocation of the corridor. In this scenario, to minimize total delay, the fixed timing plan sacrificed the traffic on Link 6. The dynamic plan for Scenario 2 produced much better results. It created green progression with dynamic bandwidths: The first three bands were of three time-intervals while the fourth one was of one time-interval. This strategy provided more green time to the traffic on Link 6. This flexibility of the dynamic plan reduced average delay by more than 10%, a drop from 72.4 seconds to 65.1 seconds.

The last comparison is the performance between the fixed and dynamic timing plans. Table 6 summarizes the reduction in delay from the dynamic timing plans for the different scenarios. It should be noted that the delays of the fixed time plans obtained here are more optimistic than their actual implementation. The calculations assume that the dynamic traffic demands are known perfectly, whereas most fixed time systems only work on historical average traffic conditions. Thus, the improvement estimates of the

Table 2 Scenario 1: Dynamic vs. Fixed Plans for Light Traffic

(A) Dynamic Plan Average Delay: 29.6 s

T	C(1,1)	C(1, 2)	C(1, 3)		C(2,1)	C(2,2)	C(2,3)		C(3.1)
1	120			XX				XX	
2	115	5		XX				—	
3	110	5	5	—				XX	
4	105	5	5	—	5			XX	
5	100	5	5	—	5	5		XX	
6	95	5	5	XX	5	5	5	—	
7	90	5	10	—		5	5	—	5
8	85	5	10	—	5		5	—	10
9	80	5	10	—	5	5		XX	15
10	75	5	10	XX	5	5	5	—	15
11	70	5	15	—		5	5	—	20
12	65	8	12	—	5		5	—	25
13	60	8	12	—	5	5		XX	30
14	55	8	12	XX	5	5	5	—	30
15	50	8	17	—		5	5	—	35
16	45	13	12	—	5		5	—	40
17	42	12	12	—	5	5		XX	45
18	37	12	12	XX	5	5	5	—	45
19	32	12	17	—		5	5	—	50
20	27	17	12	—	5		5	—	55
21	27	12	12	—	5	5		XX	60
22	22	12	12	XX	5	5	5	—	60
23	17	12	17	—		5	5	—	65
24	12	17	12	—	5		5	—	70

(B) Fixed Plan Average Delay: 29.9 s

T	C(1,1)	C(1, 2)	C(1, 3)		C(2,1)	C(2,2)	C(2,3)		C(3.1)
1	120			XX				XX	
2	115	5		XX				—	
3	110	5	5	—				—	
4	105	5	5	—	5			—	
5	100	5	5	—	5	5		XX	
6	95	5	5	XX	5	5	5	—	
7	90	5	10	—		5	5	—	5
8	85	5	10	—	5		5	—	10
9	80	5	10	—	5	5		XX	15
10	75	5	10	XX	5	5	5	—	15
11	70	5	15	—		5	5	—	20
12	65	8	12	—	5		5	—	25
13	60	8	12	—	5	5		XX	30
14	55	8	12	XX	5	5	5	—	30
15	50	8	17	—		5	5	—	35
16	45	13	12	—	5		5	—	40
17	42	12	12	—	5	5		XX	45
18	37	12	12	XX	5	5	5	—	45
19	32	12	17	—		5	5	—	50
20	27	17	12	—	5		5	—	55
21	27	12	12	—	5	5		XX	60
22	22	12	12	XX	5	5	5	—	60
23	17	12	17	—		5	5	—	65
24	12	17	12	—	5		5	—	70

1st column—time step; 2nd column—entry demand; 5th and 9th columns—signal states at A and B: "XX" red; "—" green; 10th column—arrival flow.

Table 3 Scenario 2: Dynamic vs. Fixed Plans for Asymmetrical Loadings

(A) Dynamic Plan Average Delay: 65.1 s

T	C(1,1)	C(1, 2)	C(1, 3)	A	C(2,1)	C(2,2)	C(2,3)	B	C(3.1)
1	120			XX				XX	
2	115	5		XX				—	
3	110	5	5	—				XX	
4	105	5	5	—	5			XX	
5	100	5	5	—	5	5		XX	
6	95	5	5	XX	5	5	5	—	
7	90	5	10	—		5	5	—	5
8	85	5	10	—	5		5	—	10
9	80	5	10	—	5	5		XX	15
10	75	5	10	XX	5	5	5	—	15
11	70	5	15	—		5	5	—	20
12	65	8	12	—	5		5	—	25
13	60	8	12	—	5	5		XX	30
14	55	8	12	XX	5	5	5	—	30
15	50	8	17	—		5	5	—	35
16	45	13	12	XX	5		5	—	40
17	42	12	17	XX		5		XX	45
18	37	17	17	XX			5	—	45
19	37	17	17	—				XX	50
20	37	17	12	—	5			XX	50
21	37	12	12	—	5	5		XX	50
22	32	12	12	XX	5	5	5	—	50
23	27	12	17	—		5	5	—	55
24	22	17	12	—	5		5	—	60

(B) Fixed Plan Average Delay: 72.4 s

T	C(1,1)	C(1, 2)	C(1, 3)	A	C(2,1)	C(2,2)	C(2,3)	B	C(3.1)
1	120			XX				XX	
2	115	5		—				XX	
3	110	5	5	—				XX	
4	105	5	5	—	5			XX	
5	100	5	5	XX	5	5		—	
6	95	5	10	—		5	5	—	
7	90	5	10	—	5		5	—	5
8	85	5	10	—	5	5		XX	10
9	80	5	10	XX	5	5	5	—	10
10	75	5	15	—		5	5	—	15
11	70	8	12	—	5		5	—	20
12	65	8	12	—	5	5		XX	25
13	60	8	12	XX	5	5	5	—	25
14	55	8	17	—		5	5	—	30
15	50	13	12	—	5		5	—	35
16	47	12	12	—	5	5		XX	40
17	42	12	12	XX	5	5	5	—	40
18	37	12	17	—		5	5	—	45
19	32	17	12	—	5		5	—	50
20	32	12	12	—	5	5		XX	55
21	27	12	12	XX	5	5	5	—	55
22	22	12	17	—		5	5	—	60
23	17	17	12	—	5		5	—	65
24	17	12	12	—	5	5		XX	70

1st column—time step; 2nd column—entry demand; 5th and 9th columns—signal states at A and B: "XX" red; "—" green; 10th column—arrival flow.

Table 4 Scenario 3: Dynamic vs. Fixed Plans for Jam Traffic

(A) Dynamic Plan Average Delay: 96.6 s

T	C(1,1)	C(1, 2)	C(1, 3)	A	C(2, 1)	C(2, 2)	C(2, 3)	B	C(3.1)
1	25	17	17	XX	17	17	17	XX	
2	25	17	17	XX	17	17	17	—	
3	25	17	17	XX	17	17	12	—	5
4	25	17	17	—	17	12	12	—	10
5	25	17	17	XX	12	12	12	XX	15
6	25	17	17	XX	7	12	17	—	15
7	25	17	17	XX	2	17	12	—	20
8	25	17	17	—	2	12	12	—	25
9	25	17	12	XX	5	8	12	XX	30
10	25	12	17	XX		8	17	—	30
11	20	17	17	XX		8	12	—	35
12	20	17	17	—		3	12	—	40
13	20	17	12	—	5		10	XX	45
14	20	12	12	XX	5	5	10	—	45
15	15	12	17	XX		5	10	—	50
16	10	17	17	—			10	—	55
17	10	17	12	—	5		5	XX	60
18	10	12	12	—	5	5	5	—	60
19	5	12	12	XX	5	5	5	—	65
20		12	17	—		5	5	—	70
21		12	12	—	5		5	XX	75
22		7	12	—	5	5	5	—	75
23		2	12	XX	5	5	5	—	80
24			13	—		5	5	—	85

(B) Fixed Plan Average Delay: 104.3 s

T	C(1,1)	C(1, 2)	C(1, 3)	A	C(2, 1)	C(2, 2)	C(2, 3)	B	C(3.1)
1	25	17	17	XX	17	17	17	XX	
2	25	17	17	XX	17	17	17	—	
3	25	17	17	—	17	17	12	—	5
4	25	17	17	—	17	12	12	—	10
5	25	17	17	XX	12	12	12	XX	15
6	25	17	17	XX	7	12	17	—	15
7	25	17	17	—	2	17	12	—	20
8	25	17	12	—	7	12	12	—	25
9	25	12	12	XX	7	12	12	XX	30
10	20	12	17	XX	2	12	17	—	30
11	15	17	17	—		13	12	—	35
12	15	17	12	—	5	8	12	—	40
13	15	12	12	XX	5	8	12	XX	45
14	10	12	17	XX		8	17	—	45
15	5	17	17	—		8	12	—	50
16	5	17	12	—	5	3	12	—	55
17	5	12	12	XX	5	5	10	XX	60
18		12	17	XX		5	15	—	60
19		12	17	—		3	12	—	65
20		12	12	—	5		10	—	70
21		7	12	XX	5	5	5	XX	75
22		2	17	XX		5	10	—	75
23		2	17	—			10	—	80
24		2	12	—	5		5	—	85

1st column—time step; 2nd column—entry demand; 5th and 9th columns—signal states at A and B: "XX" red; "—" green; 10th column—arrival flow.

Table 5 Scenario 4: Dynamic vs. Fixed Plans for Heavy Traffic

(A) Dynamic Plan Average Delay: 50.6 s

T	C(1,1)	C(1, 2)	C(1, 3)	A	C(2,1)	C(2,2)	C(2, 3)	B	C(3.1)
1	120	8	8	XX	8	8	8	XX	
2	115	8	13	XX	3	8	13	—	
3	110	10	17	—		8	12	—	5
4	105	15	12	XX	5	3	12	—	10
5	103	12	17	XX		5	10	XX	15
6	98	17	17	XX			15	—	15
7	98	17	17	—			10	—	20
8	98	17	12	XX	5		5	XX	25
9	98	12	17	XX		5	5	XX	25
10	93	17	17	XX			10	—	25
11	93	17	17	—			5	—	30
12	93	17	12	XX	5			XX	35
13	93	12	17	XX		5		XX	35
14	88	17	17	XX			5	—	35
15	88	17	17	—				XX	40
16	88	17	12	—	5			XX	40
17	88	12	12	XX	5	5		XX	40
18	83	12	17	XX		5	5	—	40
19	78	17	17	—			5	—	45
20	78	17	12	—	5			XX	50
21	78	12	12	XX	5	5		XX	50
22	73	12	17	XX		5	5	—	50
23	68	17	17	—			5	—	55
24	68	17	12	—	5			—	60

(B) Fixed Plan Average Delay: 56.5 s

T	C(1,1)	C(1, 2)	C(1, 3)	A	C(2,1)	C(2,2)	C(2, 3)	B	C(3.1)
1	120	8	8	XX	8	8	8	XX	
2	115	8	13	XX	3	8	13	—	
3	110	10	17	XX		8	12	—	5
4	105	15	17	—		3	12	XX	10
5	103	17	12	XX	5		15	XX	10
6	103	12	17	XX		5	15	—	10
7	98	17	17	XX		3	12	—	15
8	98	17	17	—			10	XX	20
9	98	17	12	XX	5		10	XX	20
10	98	12	17	XX		5	10	—	20
11	93	17	17	XX			10	—	25
12	93	17	17	—			5	XX	30
13	93	17	12	XX	5		5	XX	30
14	93	12	17	XX		5	5	—	30
15	88	17	17	XX			5	—	35
16	88	17	17	—				XX	40
17	88	17	12	XX	5			XX	40
18	88	12	17	XX		5		—	40
19	83	17	17	XX			5	—	40
20	83	17	17	—				XX	45
21	83	17	12	XX	5			XX	45
22	83	12	17	XX		5		—	45
23	78	17	17	XX			5	—	45
24	78	17	17	—				XX	50

1st column—time step; 2nd column—entry demand; 5th and 9th columns—signal states at A and B: "XX" red; "—" green; 10th column—arrival flow.

Table 6 Average Delay of and Percentage Difference Between the Fixed and Dynamic Timing Plans for Each Scenario

Scenario	Average Delay (s): Fixed Plan	Average Delay (s): Dynamic Plan	Reduction in Delay (%)
1	29.9	29.6	1.0
2	72.4	65.1	10.1
3	104.3	96.6	7.4
4	56.5	50.6	10.4

dynamic-timing plans obtained in this study (which is based on the availability of real-time data) are somewhat conservative. For situations with relatively light demands and without preexisting traffic, such as Scenario 1, the fixed plan performed well. Adopting a dynamic plan would add little. However, in situations with uneven cross-street demands (Scenario 2), where the network is jammed with preexisting traffic (Scenario 3), or with heavy competing demands (Scenario 4), the dynamic plan could gain substantially, as evidenced in Table 6. For Scenario 2, the dynamic plan changed the bandwidth dynamically, as discussed above. For Scenario 3, the dynamic plan used less green time for the main corridor while maintaining the same corridor throughput (Table 4). This strategy reduced the delay on the cross street and, hence, the overall average delay. For Scenario 4, the green band of the dynamic plan was wider, which increased the corridor throughput.

To illustrate further the difference between the fixed and dynamic plans, Tables 7 and 8 summarize the optimal green times for each of the four scenarios. The changes between them are not dramatic. It would be difficult and impractical to mimic each of these strategies through manual intervention to the fixed plans. These scenarios show the versatility of this dynamic formulation and the need and benefit of adopting dynamic timing plans.

4. Concluding Remarks

This study developed a dynamic traffic-control formulation, in which the entire Fundamental Diagram was considered. Traffic was modeled after the cell-transmission model (CTM), which is a numerical approximation to the LWR model. We transformed CTM to a set of mixed-integer constraints, and subsequently cast the dynamic signal control problem to a mixed-integer linear program. The significance of this transformation is that it opens up CTM to a wide range of dynamic traffic-optimization problems other than the dynamic signal-control problem developed herein.

The formulation is flexible in dealing with dynamic timing plans and traffic patterns. It can derive dynamic as well as fixed timing plans and address preexisting traffic conditions and time-dependent traffic demand patterns.

The results produced by this formulation are interesting. Contrary to the conventional wisdom that green progression does not work for congested traffic, this formulation showed that green progression could work for a wide range of demand patterns, including congested and gridlock traffic. This, however, does not say that green progression can be achieved by simply altering the offsets. It involves determining the upstream and downstream green times simultaneously, such that the initial traffic states are altered to one that would work on green progression. In

Table 7 Optimal Timing Plans for Intersection A

	Green Time for Major Corridor (s)							
	Scenario 1		Scenario 2		Scenario 3		Scenario 4	
Cycle	Dynamic	Fixed	Dynamic	Fixed	Dynamic	Fixed	Dynamic	Fixed
1	30	30	30	30	10	20	10	10
2	30	30	30	30	10	20	10	10
3	30	30	30	30	20	20	10	10
4	30	30	10	30	30	20	20	10
5	30	30	30	30	30	20	20	10
6	20	30	20	30	10	20	20	10

Table 8 Optimal Timing Plans for Intersection B

	Green Time for Major Corridor (s)							
	Scenario 1		Scenario 2		Scenario 3		Scenario 4	
Cycle	Dynamic	Fixed	Dynamic	Fixed	Dynamic	Fixed	Dynamic	Fixed
1	10	30	10	30	30	30	30	20
2	30	30	30	30	30	30	20	20
3	30	30	30	30	30	30	20	20
4	30	30	30	30	30	30	10	20
5	30	30	10	30	30	30	20	20
6	20	30	30	30	30	30	30	20

general, the results showed that a good timing plan could achieve this in just a few cycles.

The results also showed that in optimizing the system-level objective, the green-time allocation cannot be considered in an isolated manner. The demands on the neighboring junctions may influence the green allocation of a particular junction. This indicates caution for the practice of determining the green splits at the individual junction level, which could be suboptimal.

Finally, it is noted that a number of improvements are possible with this formulation. First and utmost, reducing solution time and memory requirements is an important aspect. Various heuristics are being developed at this moment. With faster solution time, one can apply the model to more complicated networks and examine whether similar conclusions can be drawn. It is also interesting to model a longer horizon to study the timing plans for transient traffic. Such improvements are necessary before this formulation can be applied to actual scenarios and to compare with existing models.

A second possible improvement is to add turning movements and bidirectional traffic to the formulation. With CTM as a platform, it is anticipated that they should be feasible without major difficulty. Ultimately, it is hoped that this new formulation will unify the earlier approaches and provide a realistic, robust platform to study traffic signal control.

Acknowledgments

This research is sponsored by the Hong Kong Research Grant Council's direct allocation grant RGC-DAG97/98.EG03 and Competitive Earmarked Research Grant HKUST6105/99E and Sino Software Research Institute Awards, SSRI98/99.EG02 and SSRI99/00.EG02. The author is also grateful for the helpful comments of an associate editor and three anonymous referees.

References

Abu-Lebdeh, G., R. Benekohal. 1997. Development of a traffic control and queue management procedure for oversaturated arterials. Transportation Research Board Annual Meeting, Paper #970707, Washington, DC.

Chang, E. 1998. Adapting a cell-based traffic control model in Hong Kong. Master of Philosophy thesis, Hong Kong University of Science and Technology, Hong Kong.

Courage, K., C. Wallace. 1991. TRANSYT/7F Users Guide, Federal Highway Administration, Washington, DC.

Daganzo, C. F. 1994. The cell-transmission model: A simple dynamic representation of highway traffic. *Transportation Res.* **28B**(4) 269–287.

———. 1995. The cell-transmission model, Part II: Network traffic. *Transportation Res.* **29B**(2) 79–93.

D'Ans, G. C., D. C. Gazis. 1976. Optimal control of over-saturated store-and-forward transportation networks. *Transportation Sci.* **10** 1–19.

Eddelbuttel, J., M. Cremer. 1994. A new algorithm for optimal signal control in congested networks. *J. Adv. Transportation* **28**(3) 275–297.

Gartner, N., S. Assmann, F. Lasaga, D. Hou. 1991. A multiband approach to arterial traffic signal optimization. *Transportation Res.* **25B** 55–74.

Gazis, D. C., 1964. Optimum control of a system of over-saturated intersections. *Oper. Res.* **12** 815–831.

Khisty, C. J., B. K. Lall. 1998. *Transportation Engineering: An Introduction*. Prentice Hall, Upper Saddle River, NJ.

Lebacque, J. P., J. B. Lesort. 1999. Macroscopic traffic flow models: A question of order. A. Ceder, ed. *Transportation and Traffic Theory.* Elsevier Science, Oxford, UK.

Lighthill, M. J., J. B. Whitham. 1955. On kinematic waves. I. Flow movement in long rivers. II. A theory of traffic flow on long crowded roads. *Proc. of Royal Society* **A229** 281–345.

Lin, W. H., D. Ahanotu. 1995. Validating the basic cell transmission model on a single freeway link. Technical note, UCB-ITS-PATH-TN-95-3, University of California, Berkeley, CA.

Little, J., M. Kelson, N. Gartner. 1981. MAXBAND: A program for setting signals on arteries and triangular networks. *Trans. Res. Record* **795** 40–46.

Lo, H. 1999a. A dynamic traffic assignment formulation that encapsulates the cell-transmission model. A. Ceder, ed. *Transporation and Traffic Theory*, 327–350. Elsevier Science, Oxford, UK.

———. 1999b. A novel traffic signal control formulation. *Trans. Res.* **33A** 433–448.

———, E. Chang, Y. C. Chan. Dynamic Network Traffic Control. *Trans. Res. A*, forthcoming.

May, D. 1990. *Traffic Flow Fundamentals*. Prentice Hall, Englewood Cliffs, NJ.

McShane, W. R., R. P. Roess, E. S. Prassas. 1998. *Traffic Engineering*. Prentice Hall, Upper Saddle River, NJ.

Michalopoulos, P., G. Stephanopoulos. 1977. Over-saturated signal systems with queue length constraints–I. Single intersection–II. Systems of intersections. *Trans. Res.* **11** 413–428.

Nagel, K., M. Schreckenberg. 1992. A cellular automaton model for freeway traffic. *J. Phys. I France* **2** 2221–2229.

Newell, G. F. 1989. Theory of highway traffic signals. Course Notes UCB-ITS-CN-89-1, University of California, Berkeley, Berkeley, CA.

———. 1991. A simplified theory of kinematic waves. Research Report UCB-ITS-RR-91-12, University of California, Berkeley, CA.

Papageorgiou, M., Hadj-Salem, H., Blosseville, M. 1990. Modelling and real-time traffic control of traffic flow on the Boulevard Peripherique in Paris. IFAC Control, Computers, Communications in Transportation, Paris, France 205–211.

Richards, P. I. 1956. Shockwaves on the highway. *Oper. Res.* **4** 42–51.

Smilowitz, K. R., C. F. Daganzo. 1999. Predictability of time-dependent traffic backups and other reproducible traits in experimental highway data. Working Paper UCB-ITS-PWP-99-5, California PATH Program, Institute of Transportation Studies, University of California, Berkeley, CA.

Stephanopoulos, G., P. Michalopoulos, G. Stephanopoulos. 1979. Modelling and analysis of traffic queue dynamics at signalized intersections. *Trans. Res.* **13A** 295–307.

Texas Transportation Institute (TTI). 1991. *PASSER II-90 Microcomputer User's Guide.* Texas A&M University, College Station, TX.

Wallace, C. E., K. G. Courage, M. A. Hadi, A. C. Gan. 1998. *TRANSYT-7F User's Guide*. U.S. Department of Transportation Federal Highway Administration. Washington, DC.

Wey, W., R. Jayakrishnan. 1997. A network traffic signal optimization formulation with embedded platoon dispersion simulation. Transportation Research Board Annual Meeting Paper #971337. Washington, DC.

Wood, K. C. 1993. Urban traffic control systems review. Transport Research Laboratory Project Report 41. Berkshire, UK.

(Received: February 1999; revisions received: September 1999, July 2000; accepted: July 2000).